Vol. 05, No. 4 (2023) 591-600, doi: 10.24874/PES05.04.001

Proceedings on Engineering Sciences

www.pesjournal.net

ROLE OF MARTENSITE FORMATION ON CYCLIC STRESS-STRAIN BEHAVIOR OF 304LN-STAINLESS STEEL

Chandra Kant
Gulam Ashraful Harmain[1]

Received 25.05.2023.
Accepted 12.09.2023.
UDC – 539.431

Keywords:

Cyclic Deformation-Induced Martensite, Cyclic Stress-Strain Response, Low cycle fatigue, Austenitic Stainless Steel 304LN (0.11%).

A B S T R A C T

In this investigation, experiments have been carried out at room temperature (RT); 300K, and at high temperature (HT); 573K to determine the role of martensite formation in the strain-controlled low cycle fatigue of 304LN (0.11%) stainless steel. Deformation-induced martensite was significantly present (0.7 to 2.3%) for RT, however, in trace amounts (0.05 to 0.07%) at HT. The presence of deformation-induced martensite at RT had detrimental effect on low cycle fatigue life of 304LN-SS. Significant drop in stress level was observed at HT (270-407 MPa) compared to value of stress at RT (395-493 MPa) for cyclic stain amplitude values in the range (0.5 to 1.1%). The number of reversals to failure decreased with increasing strain amplitude (0.5 to 1.1%) from 17540.0 to 1046.0 at RT while at HT the number of cycles to failure decreased (15562 to 700). The maximum number of hardening cycles was found to increase from 15 to 55 for a temperature rise from 300K to 573K. The beneficial improvement in cyclic stress-strain response (hardening cycles) at 573K is attributed to absence of martensite. Effects of deformation-induced martensite and temperature have been invoked to account for changes that have been observed in the cyclic stress-strain behavior.

1. INTRODUCTION

The nuclear power industry relies heavily on austenitic stainless steels such as 304LN-SS, owing to its corrosion resistance and other desirable mechanical properties such as ductility and strain hardening. One of the candidate material for the pipeline of the advanced deuterium oxide (D_2O) based nuclear power plant is the austenitic grade 304LN stainless steel (Belyakov et al., 2000; Rowcliffe et al., 1998). In such a system temperature variations up to 423K occur between the hot and cold branches of mixing tees, that may induce thermal shocks in the pipes. In articles (G.A. Harmain, 2005; Kant & Harmain, 2021a, 2021b, 2021c) several in-service loadings were discussed in detail.

Strain amplitude fatigue curves are required as per design standards such as ASM and the French RCC-M code (Rowcliffe et al., 1998) to assess the in-service integrity of such structures. Evaluation of material's resistance to low cycle fatigue (LCF), uses strain-controlled experiments (also known as plastic strain-controlled testing).

[1] Corresponding author: Gulam Ashraful Harmain
Email: gharamain@nitsri.ac.in

304LN is a metastable austenitic stainless steel, undergoes a phase change (austenite to martensite) during the deformation process, which is a function of several parameters such as strain amplitude, strain rate, the elemental composition of the material, and level of deformation (Kumar & Singhal, 1989). It has been found that the extent of strain amplitude at room temperature (RT) influences martensite formation (by the deformation-induced martensite process) (Ahmedabadi et al., 2016; Das et al., 2016; Dey et al., 2016; Gonchar et al., 2018; Krupp et al., 2008; Liu et al., 2017; Paul et al., 2018; Pegues et al., 2017). Martensite development may inhibit plastic deformation in austenitic stainless steels such as 304L-SS (Ganesh Sundara Raman & Padmanabhan, 1995), which influences deformation behavior and hence the cyclic stress-strain response of components.

Significant research has been reported on the 304L-SS cyclic deformation behavior (Baudry & Pineau, 1977; Bayerlein et al., 1989; Belyakov et al., 2000; Dey et al., 2016; Gonchar et al., 2018; Liu et al., 2017; Paul et al., 2018; Pegues et al., 2017; Rowcliffe et al., 1998; Juho Talonen et al., 2005) but there is limited data available on the cyclic deformation behavior of austenitic stainless steel 304LN-(0.11%)- SS.

The present investigation is focused to analyze the effect of formation of martensite on the cyclic stress-strain response of 304LN-SS at room temperature (RT=300K) and high temperature (HT= 573K). The study also provides low cycle fatigue life with synergetic effect of cyclic deformation and temperature with wide range of strain amplitudes (0.5 to 1.1%) that have been used to study martensite formation.

2. MATERIAL AND METHOD

Plates made of 304LN-SS with a thickness of 20 millimeters were utilized in the present investigation. Microstructure of the material is shown in Figure. 1. The chemical composition of the material is presented in Table 1.

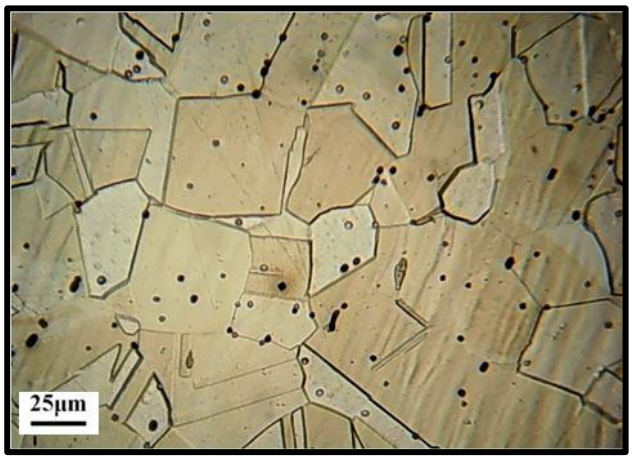

Figure 1. Microstructure of 304LN-SS

Table 1. Chemical composition of 304LN-SS.

Element	C	Si	Ni	Cr	Cu	N	Fe
Weight (%)	0.027	0.5	8.1	18.3	0.3	0.11	Balance

The geometry of the sample used is shown in Figure.2 (a). Tensile tests on these samples were conducted in laboratory air at strain rates of $1*10^{-3}$ s^{-1} at 300K (RT) and 573K (HT) using a servo-hydraulic universal testing machine of Walter + Bai Ag as shown in Figure. 2(b). Tensile stress-strain curves were obtained using Tinious Olsen, universal testing machine.

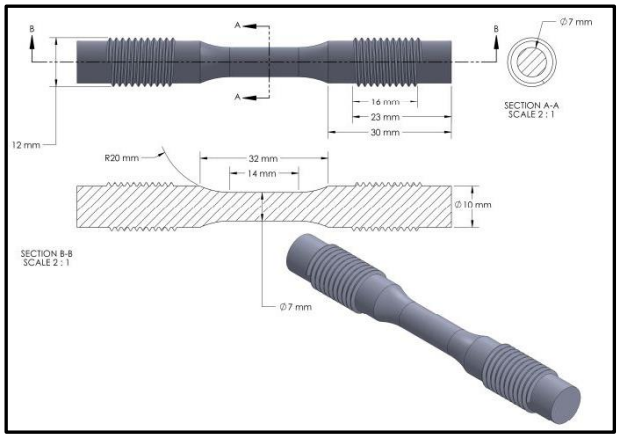

(a)

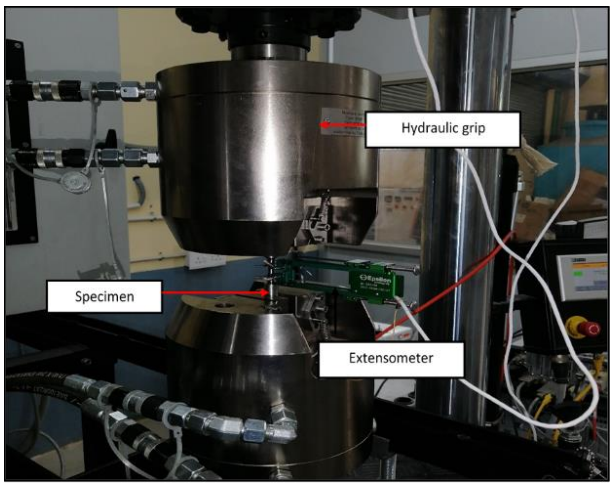

(b)

Figure 2. (a) Detailed geometry of specimen used in the present investigation. (b) Experimental setup (Walter +Bai Ag) used for conducting LCF tests

Low cycle fatigue (LCF) experiments have been conducted on Walter + Bai Ag fatigue testing machine-100 kN as shown in Figure. 2(b). Several strain amplitudes of 0.5%, 0.8%, 1.0%, and 1.1% were used at room temperature (RT; 300K) and high temperature (HT; 573K) in the current investigation. Axial deformation was measured using a 12.5 mm extensometer. The strain rate was maintained at $1*10^{-3}$ s^{-1} for LCF tests. The experiments were deemed to have finished when either the specimen broke or the load dropped by 25%, whichever was earlier.

3. RESULTS AND DISCUSSIONS

3.1 Effect of temperature on tensile behavior

Tensile tests were conducted to obtain the influence of temperature on the mechanical properties of the material at RT and HT. Tensile properties such as yield strength and ultimate strength dropped appreciably *i.e.*, by 28 and 32% respectively. Ductility decreased significantly *i.e.*, by 43% with respect to room temperature value shown in Figure. 3. The counterintuitive behavior of ductility at elevated temperature is attributed to significantly reduced level of deformation-induced martensitic phase transformations (which will be quantified and discussed further in subsequent sections). The experimental results corroborate well with the result of the reference (Byun et al., 2004).

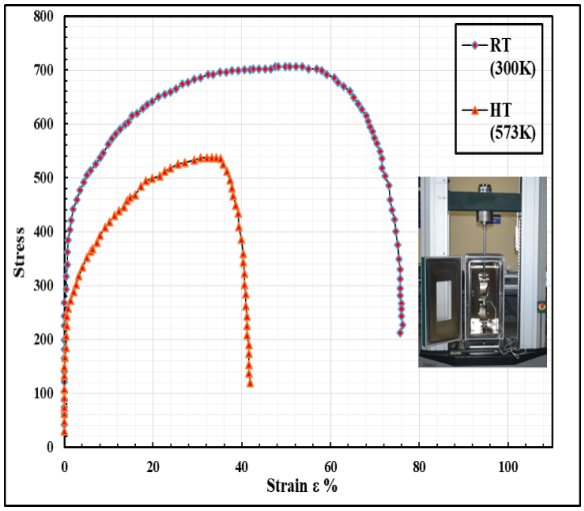

Figure 3. Monotonic stress-strain curve, obtained using Tinius Olsen UTM

3.2 LCF at room temperature (RT) and high temperature (HT)

The Coffin-Manson relationship was invoked to obtain fatigue life (N_f), *i.e.*, ($2N_f$) reversals. The plastic strain amplitude ($\frac{\Delta\epsilon_P}{2}$), and the number of reversals($2N_f$), are related through fatigue ductility coefficient ($\varepsilon_{f'}$) and fatigue ductility exponent (c) as: $\frac{\Delta\epsilon_P}{2} = \varepsilon_{f'}(2N_f)^c$. Low cycle fatigue (LCF) life variation with plastic strain amplitude ($\frac{\Delta\epsilon_P}{2}$) is shown in Figure. 4, for 304LN stainless steel based on Coffin–Manson equation

It is observed that the low cycle fatigue life of 304LN-SS was consistently lower at high temperature (HT=573K) than at room temperature (RT=300K), for all the strain amplitudes (0.5 to 1.1%) considered in this study. The slope of low cycle fatigue life at RT and HT are -0.327 and -0.298 respectively.

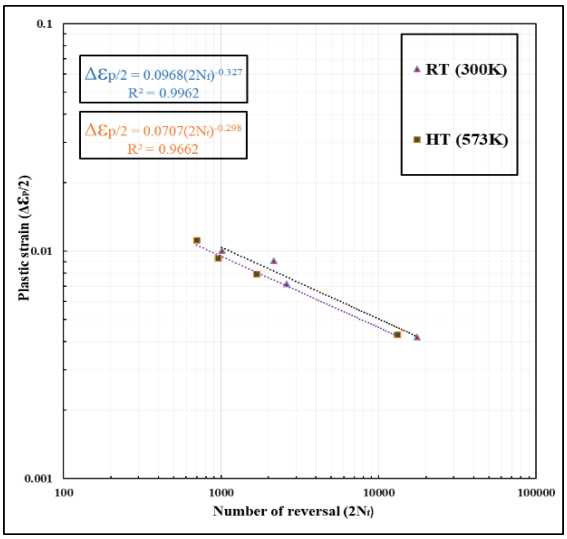

Figure 4. Plastic strain amplitude versus number of reversals ($2N_f$) (at RT (300K) and HT (573 K)

The variation in the slope of plastic strain amplitude with respect to number of reversals at RT(300K) and HT(573K) is attributed to microstructural and sub-structural changes that have occurred in the material during deformation process (Berling et al., n.d.). Such variations in plastic strain amplitude have been reported for multi-phase steels (Mediratta et al., 1986; Radhakrishnan, 1992) and Al-Li alloys (Mediratta et al., 1986; Radhakrishnan, 1992). Coffin–Manson low cycle fatigue has been studied on the basis of thermal activation energy of dislocation motions (Kim et al., 2009) in the case of cast austenitic steels.

3.3 Fracture surface examination

LCF fractured samples were examined to observe the microscopic features using the Scanning Electron Microscope. In Figure. 5 (a)-(d) and 6(a)-(d), details of fractographs of samples for strain amplitude (0.5 to 1.1%) for RT (300K) and HT (573K) respectively are provided. It is observed from Figure. 5(a)-(d) that prominent features of metal matrix damage are manifested in the form of striations spacing marked by the green rectangles. It is conspicuous that striations have wider spacing as strain amplitude is increased from (0.5-1.1%). Another feature of the fractured surfaces has been given by red rectangular boundaries showing secondary cracks. It is also observed in Fig. 5 (b) to (d) that martensite transformation is also present. The martensite phase is identified by smooth facets which have started to appear in Figure. 5(b) to Fig. 5(d).The martensite facets are proportionately larger at higher values of strain amplitude. Thus cyclic deformation induced martensite transformation (shown by red color arrows in Figure. 5(b),(c), and (d) are attributed as a factor for anomalous behavior of increased ductility at room temperature, compared with ductility at elevated temperature (573K). The presence of martensite significantly affects cyclic stress-strain response at room temperature.

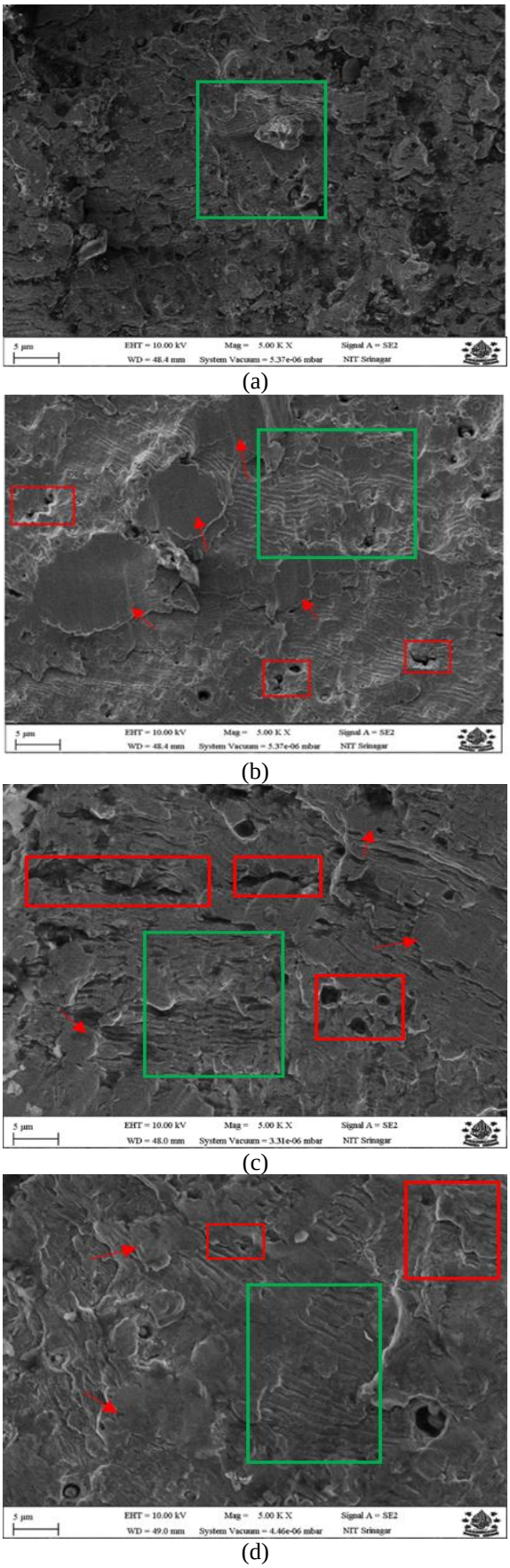

Figure 5. Low cycle fatigue, fractured samples at RT. (a) at 0.005 strain amplitude. (b) at 0.008 strain amplitude. (c) 0.01 strain amplitude. (d) 0.011 strain amplitude

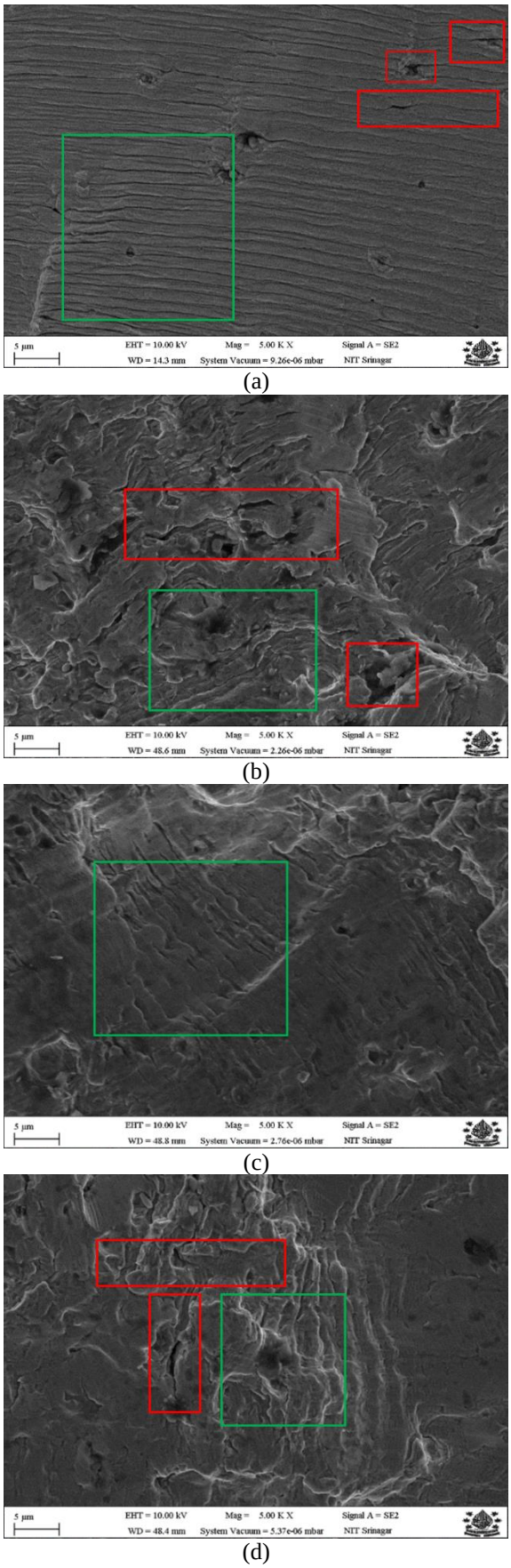

Figure 6. Low cycle fatigue, fractured samples at HT. (a) at 0.5% strain amplitude. (b) at 0.8% strain amplitude. (c) 1% strain amplitude. (d) 1.1% strain amplitude

The fractured surfaces of samples at high temperature (573K) at strain amplitudes of (0.5, 0.8, 1.0and 1.1%) are shown in Figure. 6(a), (b), (c), and (d) respectively. In Figure. 6(a) classical striation spacings are succinctly visible in the entire area (some typical portion has been shown by the green rectangle) with some damage in the form of secondary cracks (shown by red rectangles). In Fig. 6(b) the damage to metal matrix by secondary cracks is significant (shown by red rectangles), while the striations are mitigated to some extent in some locations (as shown by green rectangle).

In Figure. 6(c) the damage to the material is prominent and the spacings of striations have also become wider (shown by green rectangle) and elsewhere the striations are mitigated. In Figure. 6(d) at the highest value of strain amplitude (0.11%) the accumulated damage to the metal matrix through de-cohesion and secondary cracks is demarcated by red rectangles. The striations have become very wide and prominent (as shown by green rectangle).

3.4 Effects of Temperature

The stress variation with increasing number of cycles at strain amplitudes of 0.5%, 0.8%, 1%, and 1.1% has been shown in Figure. 7(a) and 7(b) at room temperature (300K) and elevated temperature (573K) respectively.

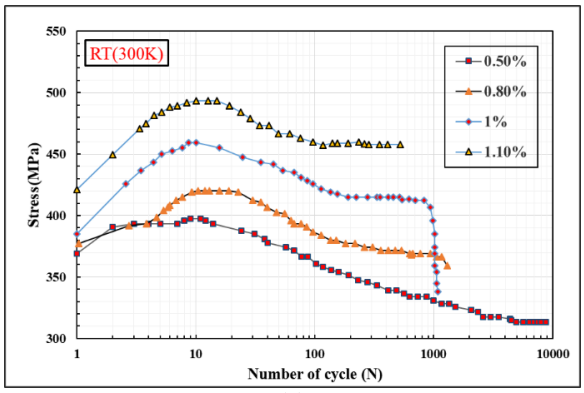

(a)

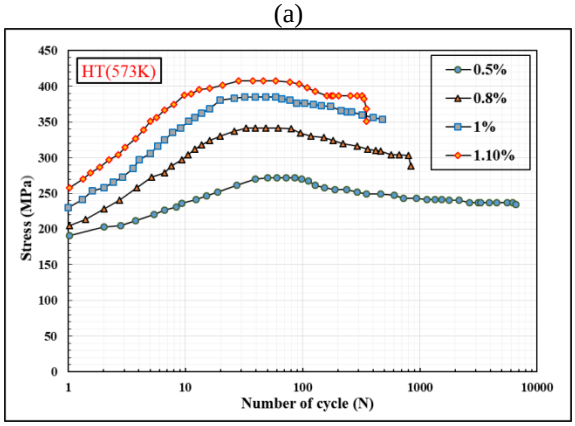

(b)

Figure 7. Stress response for several strain amplitudes (0.5 -1.1%). (5a) at RT. (5b) at HT

It is observed in Figure 7(a) that for first 10 to 15 cycles there is cyclic hardening at room temperature and subsequently cyclic softening for all strain amplitude. At elevated temperature (573K) hardening occurs up to 55 cycles which is then followed by gradual softening till failure. At room temperature, larger response stress occurs for all the strain amplitude considered. The initial hardening slopes at high temperature (573K) were found steeper than for room temperature conditions for the same strain amplitude values. Since the softening at elevated temperature does not exhibit steady-state therefore subsequent analysis has considered half-life ($N_f/2$) cycle instead of steady state. The hardening and softening of material 304LN SS is directly related to changes in microstructure and substructure as a result of cyclic deformation.

In virgin 304LN-SS microstructure was 100% austenite as depicted in Figure. 1. SEM fractographs of samples at RT (300K), reveal the presence of deformation-induced martensite as shown in Figure. 8, at some locations (shown by symbols X, Y, and Z) however, martensite is not present at elevated temperature (573K) samples shown in Figure. 9.

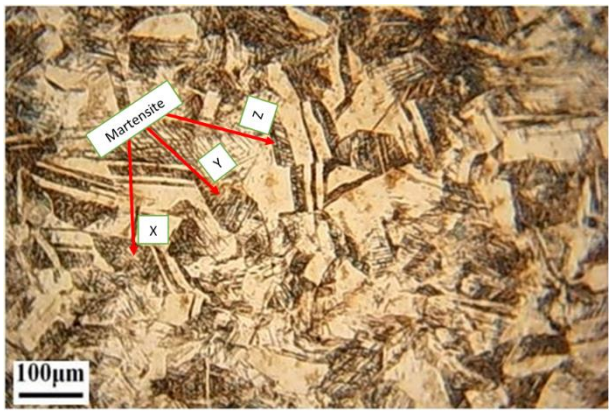

(a)

Figure 8. Microstructure of 304LN-SS after sample failure at RT (300K) and 1.1% strain amplitude

Figure 9. Microstructure of 304LN-SS after sample failure at HT (573K) and 1.1% strain amplitude

Transformation of austenite to martensite in microstructure is a function of strain rate, temperature, and applied strain (Lee et al., 2022). In particular strain range, the hardening and softening may be attributed to the influence of temperature as is evident in Figure. 7(a) and 7(b). Even though the material shows initial hardening for the first 15 to 20 cycles at RT and 30 to 55 cycles at HT (573K), the levels of stress that is necessary to deform the material at 573K is substantially lower than at 300K. Plastic damage (response to strain) is primarily attributed to two factors, the formation of dislocations and their mobility (Hartmaier et al., 2005). Barriers such as grain boundary, precipitates, phase transformations, and dislocations and their interaction with one another also affects the response stress.

304LN–SS is metastable austenitic stainless steel at room temperature (300K), therefore it shows austenite to martensite phase transformation under the influence of deformation (tensile, compressive, shear deformation, *etc*.). Deformation-induced martensitic transformation (DIMT) also affects the dislocation motion. In (Bayerlein et al., 1989), it is reported that the martensitic transformation that occurs in stainless steel 304LN-SS under cyclic stress at room temperature effectively reduces plastic deformation. As a result of limited plastic deformation due to DIMT, it is expected that higher level of stress will occur at RT for the same level of applied strain. When 304LN-SS is deformed (axial cyclic strain) at room temperature, pure austenitic phase 304LN-SS is transformed into two phases (austenite + martensite) by DIMT, while at HT (573 K) 304LN-SS is stable (573 K $>M_{d30}$), (where M_{d30} is the temperature at which 50% austenite will convert to martensite by DIMT in metastable steels due to 30% deformation)(Bayerlein et al., 1989). Hence microstructural phase is unaltered by deformation at elevated temperature (573K) however, pure austenitic phase is strong enough to sustain cyclic deformation (Byun et al., 2004; Krupp et al., 2008; Kumar & Singhal, 1989; Juho Talonen et al., 2005).

This microstructural alteration *i.e.,* DIMT has a substantial influence on the mechanical response (yield stress, tensile stress, elongation percentage) of 304LN-SS which is also evident in Figure. 3 (for monotonic stress-strain response) where yield strength, ultimate strength, and elongation decreased by 28%, 32%, and 43% respectively. Since temperature plays a major role in the stability of austenite, the decrease in elongation by 43% beyond 300K is attributed to formation of martensite at room temperature. Feritscope was used for identification of martensite at RT (300K) and HT (573K) as is shown in Figure. 8. DIMT has a significant impact on the tensile properties such as strain hardening and ductility of the material (Byun et al., 2004). The fall in material strength and elongation at elevated temperature has also been reported for ASS (300 series) by (Byun et al., 2004). The results of reference (Nagy et al., 2004) (J. Talonen & Hänninen, 2007) corroborate well with the result of the present study. The role of martensite has also been studied for 300 austenitic stainless steel by (J. Talonen & Hänninen, 2007; Weiß et al., 2006) and is in conformity with the findings of the present investigation.

It has been observed that transformation from the austenite phase to the martensite, occurred at a RT during cyclic loading with strain amplitude (0.5%, 0.8%, 1.0%, and 1.1%). Cyclic deformation-induced martensite had higher strength than the austenitic phase. This is the key factor responsible for change in properties in the cyclic stress response that was observed at 300 K and 573 K in Figure. 7a and 7b respectively. In (Krupp et al., 2008),(Nagy et al., 2004) it was reported that the low cycle fatigue behavior of austenitic stainless steel at temperatures ranging from -100 to 300 K, the cyclic hardening increased as the temperature decreased. This was attributed to deformation-induced martensite transformation (DIMT) that increased as the temperature decreased.

An in-depth investigation into the microstructural changes brought by LCF using a feritscope and optical microscope is presented in Table 2, that presents DIMT at room temperature and elevated temperature respectively.

Table 2. Strain-induced martensite and failure cycles for various levels of strain amplitudes.

Room temperature 300 K			High temperature 573 K		
Strain %	N_f (cycles to failure)	Martensite %	Strain %	N_f (cycles to failure)	Martensite%
0.5%	8770	0.7%	0.5%	7781	0.05%
0.8%	1297	1.1%	0.8%	1023	0.04%
1.0%	1083	1.9%	1.0%	1440	0.05%
1.1%	523.00	2.3%	1.1%	350	0.07%

The feritscope readings were obtained for HT samples which showed quite trace amount of martensite (0.04 to 0.07%). However, the percentage of martensite at room temperature (300K) is 0.7 to 2.3% that results in higher response stresses. High temperature leads to the activation of thermal processes, that makes dislocations to glide easily that decreases the resistance to material flow that results in lower response stresses. The stress response of 304LN-SS at 573K is in conformity with (*Yamaguchi K, Kanazawa K. Electron Microscope on Deformati... - Google Scholar*, n.d.). Low cycle fatigue tests carried out by (*Yamaguchi K, Kanazawa K. Electron Microscope on Deformati... - Google Scholar*, n.d.) on austenitic stainless steel 316 at elevated temperature demonstrated the presence of organized dislocation arrays that lead to lower elastic strain energies in comparison to cellular arrangements.

Deformation-induced martensite affects cyclic stress-strain curve, which is controlled by cyclic changes in hardness (315 to 210 Hv) and ductility and both were found to decrease with increasing temperature (300 to 573K). Response stress increased with the increase in hardness.

The overall strain amplitude for the hysteresis loop may be expressed as: $\frac{\Delta\varepsilon_T}{2} = \frac{\Delta\varepsilon_e}{2} + \frac{\Delta\varepsilon_P}{2}$ where $\frac{\Delta\varepsilon_T}{2}$, $\frac{\Delta\varepsilon_e}{2}$ and $\frac{\Delta\varepsilon_p}{2}$ are total, elastic, and plastic strains amplitudes respectively. Strain ratio (SR) = $\frac{\Delta\varepsilon_p}{\Delta\varepsilon_e}$, in fatigue loading is an indicator of hardening and softening. In Figure. 10(a) and 10(b) it is observed that the value of SR decreases until hardening behavior exists (which is the number of hardening cycles 15 to 20 for RT and 30 to 55 for HT). It is evident in Figures 10(a) and 10(b) respectively, that the value of SR decreased till-hardening behavior which validated the hardening cycles for both RT and HT.

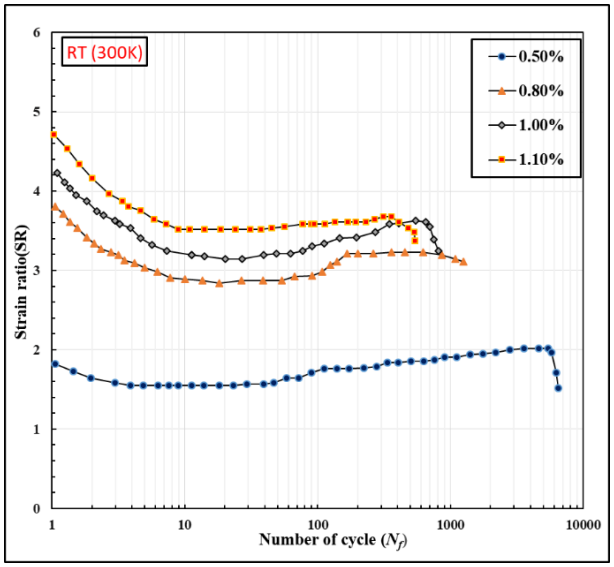

(a)

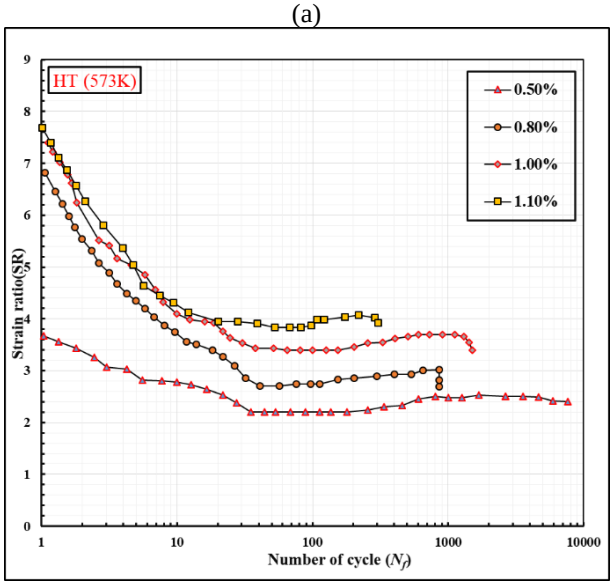

(b)

Figure 10. Strain ratio variation with an accumulation of fatigue damage. (a) at 300K. (b) at 573K

The material displayed softening and stable behavior till failure beyond the number of hardening cycles. The patterns of SR were similar for all strain ranges at RT and HT, although the magnitude of SR (3.6 to 7.6) at 573K was conspicuously higher than at 300K. SR values were in the range of (1.8 to 4.7) at 300K, which manifested as high plastic strain at elevated temperature than room temperature which was during the first 10-cycles rate of SR was in the range of (0.147 to 0.34) for 300K, while for 573K SR values are in the range of (0.028 to 0.11) at strain amplitudes (1.1 to 0.5%) as shown in Figures 10 (a) and 10 (b) respectively.

Figure. 11 gives the cyclic stress-strain response for 304LN-SS for the first cycle at 300K and 573K respectively. In these hysteresis loops it is observed that the proportion of plastic strain amplitude was significantly higher for 573K. The higher value of plastic strain amplitude which is observed at 573K is a result of dislocation network formation and ease of movement of dislocations.

Figure. 11 shows that in the HT hysteresis loop (compared to the RT hysteresis loop), the proportion of plastic strain amplitude was significantly larger for the first cycle. More plastic strain amplitude that is observed at 573K is the result of both the significant dislocation formation as well as the ease of movement of the dislocation.

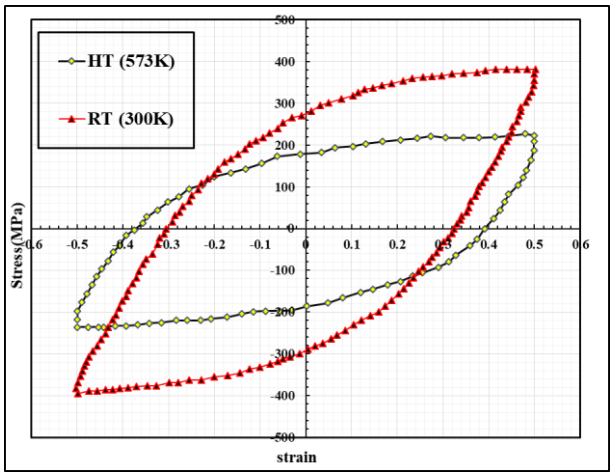

Figure 11. Cyclic stress-strain response of 304LN-SS for the first cycle

Strain amplitudes from 0.5 to 1.1% show limited dislocation motion because of higher plastic strains. Dislocation piles up and entanglements in successive cycles take place as a direct result of higher plastic strains. Therefore more hardening cycles occur in 304LN (1.1%)-SS at HT.

3.5 Cyclic stress-strain

The cyclic stress-strain (CSS) curves have been generated using the peak stresses and strains of the half-

life cycles (stabilized loop). The cyclic stress-strain curve is obtained using equation 1 as:

$$\frac{\Delta\varepsilon}{2} = \frac{\Delta\sigma}{2E} + \left[\frac{\Delta\sigma}{2K'}\right]^{\frac{1}{n'}} \quad (1)$$

where $\Delta\sigma$ and $\Delta\varepsilon$ are the stress amplitude and total strain amplitude respectively, E is the modulus of elasticity, K' is the cyclic strength coefficient and $1/n'$ is the cyclic strain hardening exponent.

Figure. 12 (a) and (b) show the CSS curves for RT and HT respectively, at various strain amplitudes (0.5 to 1.1%).The monotonic stress strain curve have also been shown along with CSS curves for RT (300K) and HT (573K) respectively. The cyclic and monotonic hardening exponent for 304LN-SS is presented in Table. 3.

The material shows cyclic hardening or softening when the stress-strain cycle are above or below the monotonic stress-strain curve respectively. Figure. 12 (a) shows that for smaller strain amplitudes, the monotonic curve is higher than the cyclic stress strain curves at RT.

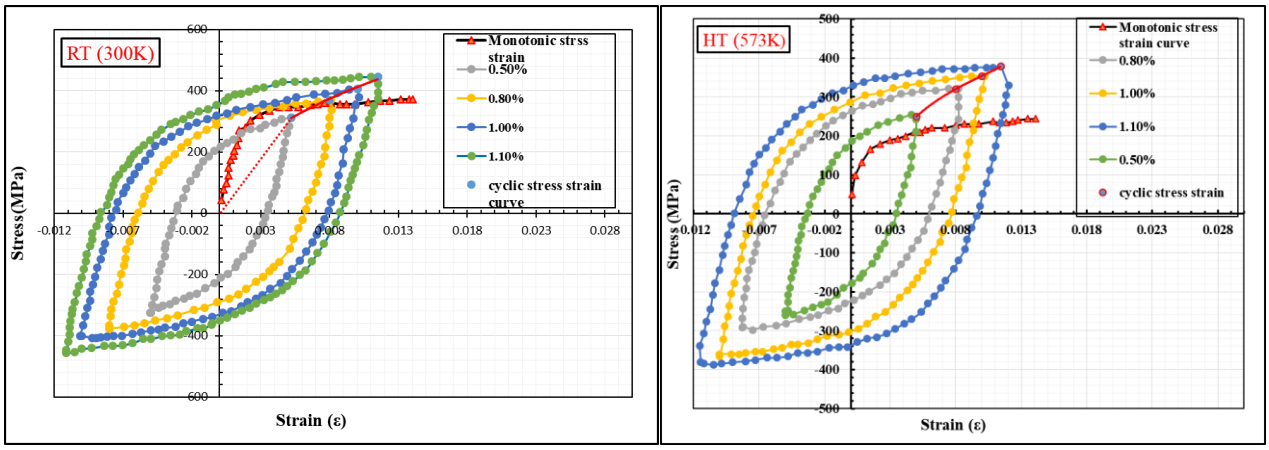

(a) (b)

Figure 12. Monotonic and cyclic stress-strain response. (a) At RT. (b) At HT

Table 3. Effect of temperature on cyclic hardening parameters of 304LN-SS.

Conditions	Cyclic hardening parameters	Numerical value	Monotonic hardening parameter	Numerical value
RT (300K)	K'	2989.5	K	673.15
	$1/n'$	2.4846	1/n	7.7025
HT (573K)	K'	5801	K	691.83
	$1/n'$	1.7393	1/n	5.98

This shows that the material softens under cyclic loading. In the transition zone, the CCS curve goes above the monotonic curve, as the strain amplitude is increased, and the material has a tendency to cyclically harden. Figure. 12 (b) shows that at HT, the CSS curve is always above the monotonic stress-strain curve.

At room temperature, initially, for 10 to 20 cycles, the material shows hardening behavior followed by softening, initial hardening (high peak stress) can be attributed to DIMT, which increases the hardness that manifests as high stress and less number of hardening cycles. In the case of HT, the stable austenite phase stops the martensitic transformation, causing the material to become less hard. In comparison to the first 10 to 20 cycles at RT, hardening persists larger number of cycles (*i.e.*, 30 to 55 cycles. The monotonic curve for RT has peak stress of 370MPa for 1.1% strain amplitude, where two gliding systems may operate simultaneously for dislocation motion. At high temperatures, the monotonic stress-strain curve barely reaches 233 MPa, indicating that one gliding system is available for dislocation motion leading to hardening.

4. CONCLUSIONS

In this study, influence of deformation induced martensite on cyclic stress strain response was evaluated at room temperature (RT) and high temperature (HT).

1. The contribution of plastic strain is (1.58596 to 9.579%) more at HT (573 K) than RT (300 K) for applied strain amplitude (0.5% to 1.1%), while in unidirectional loading material shows 43% higher ductility at RT than HT, that is a manifestation of deformation induced martensite. The proportion of martensite was 0.07 to 2.3% at RT while at HT the level of martensite was 0.05 to 0.07% for strain amplitudes of 0.5 to 1.1%.

2. Less hardening cycles (10-15) and high response stress at RT was observed while at HT corresponding hardening cycles were (30-55) for several strain amplitudes (0.5% to 1.1%) is also attributed to deformation-induced martensite and thermal activation of material.
3. Low cycle fatigue life was found to decrease (24.91 to 30.69 %) with an increase in strain amplitude (0.5 to 1.1%) and temperature rise (300 to 573K).

Acknowledgement: We acknowledge director NIT Srinagar to provide access to Mechanics of Material laboratory to conduct experiments.

References:

Ahmedabadi, P. M., Kain, V., & Agrawal, A. (2016). Modelling kinetics of strain-induced martensite transformation during plastic deformation of austenitic stainless steel. *Materials & Design*, *109*, 466–475. https://doi.org/10.1016/J.MATDES.2016.07.106

Baudry, G., & Pineau, A. (1977). Influence of strain-induced martensitic transformation on the low-cycle fatigue behavior of a stainless steel. *Materials Science and Engineering*, *28*(2), 229–242. https://doi.org/10.1016/0025-5416(77)90176-8

Bayerlein, M., Christ, H. J., & Mughrabi, H. (1989). Plasticity-induced martensitic transformation during cyclic deformation of AISI 304L stainless steel. *Materials Science and Engineering: A*, *114*(C), L11–L16. https://doi.org/10.1016/0921-5093(89)90871-X

Belyakov, V. A., Fabritsiev, S. A., Mazul, I. V., & Rowcliffe, A. F. (2000). Status of international collaborative efforts on selected ITER materials. *Journal of Nuclear Materials*, *283–287*(PART II), 962–967. https://doi.org/10.1016/S0022-3115(00)00233-6

Berling, J., Symposium, T. S.-F. at H. T. A., & 1969, U. (n.d.). Effect of Temperature and Strain Rate on Low-Cycle Fatigue Resistance of AISI 304. *Books.Google.Com*.

Byun, T. S., Hashimoto, N., & Farrell, K. (2004). Temperature dependence of strain hardening and plastic instability behaviors in austenitic stainless steels. *Acta Materialia*, *52*(13), 3889–3899. https://doi.org/10.1016/J.ACTAMAT.2004.05.003

Das, Y. B., Forsey, A. N., Simm, T. H., Perkins, K. M., Fitzpatrick, M. E., Gungor, S., & Moat, R. J. (2016). In situ observation of strain and phase transformation in plastically deformed 301 austenitic stainless steel. *Materials & Design*, *112*, 107–116. https://doi.org/10.1016/J.MATDES.2016.09.057

Dey, R., Tarafder, S., & Sivaprasad, S. (2016). Influence of phase transformation due to temperature on cyclic plastic deformation in 304LN stainless steel. *International Journal of Fatigue*, *90*, 148–157. https://doi.org/10.1016/J.IJFATIGUE.2016.04.030

G.A. Harmain. (2005). An investigation on single overload fatigue crack growth retardation, Part-2 (Crack closure decomposition)). *Journal of Metallurgy and Materials Science*, *47*(4), 189–197.

Gamri, H., Allaoui, O., & Zidelmel, S. (2021). Microstructural and Tribological Characterization of API X52 Dual-phase Steel. *Tribology in Industry*, *43*(4), 632–642. https://doi.org/10.24874/ti.1098.04.21.11

Ganesh Sundara Raman, S., & Padmanabhan, K. A. (1995). A comparison of the room-temperature behaviour of AISI 304LN stainless steel and Nimonic 90 under strain cycling. *International Journal of Fatigue*, *17*(4), 271–277. https://doi.org/10.1016/0142-1123(95)93539-E

Gonchar, A. V., Mishakin, V. V., & Klyushnikov, V. A. (2018). The effect of phase transformations induced by cyclic loading on the elastic properties and plastic hysteresis of austenitic stainless steel. *International Journal of Fatigue*, *106*, 153–158. https://doi.org/10.1016/J.IJFATIGUE.2017.10.003

Hartmaier, A., Buehler, M. J., & Gao, H. (2005). Two-dimensional discrete dislocation models of deformation in polycrystalline thin metal films on substrates. *Materials Science and Engineering: A*, *400–401*(1-2 SUPPL.), 260–263. https://doi.org/10.1016/J.MSEA.2005.03.069

Kant, C., & Harmain, G. A. (2021a). A Model Based Study of Fatigue Life Prediction for Multifarious Loadings. *Key Engineering Materials*, *882*, 296–327. https://doi.org/10.4028/WWW.SCIENTIFIC.NET/KEM.882.296

Kant, C., & Harmain, G. A. (2021b). An Investigation of Constant Amplitude Loaded Fatigue Crack Propagation of Virgin and Pre- Strained Aluminium Alloy. *International Conference on Advanced Manufacturing and Materials Processing*, 1–14.

Kant, C., & Harmain, G. A. (2021c). Fatigue Life Prediction Under Interspersed Overload in Constant Amplitude Loading Spectrum via Crack Closure and Plastic Zone Interaction Models - A Comparative Study. *9th International Conference on Fracture Fatigue and Wear (FFW 2021)*, 1–10.

Khoma, M., Zakiev, V., Vynar, V., Vasyliv, C., Datsko, B., & Golovchuk, M. (2022). Influence of Heat Treatment of 30MnB5 Steel on its Micromechanical Properties and Resistance to Abrasion Wear. *Tribology in Industry*, *44*(1), 310–321. https://doi.org/10.24874/ti.1146.06.21.02

Kim, Y. J., Jang, H., & Oh, Y. J. (2009). High temperature low cycle fatigue properties of a HF30-type cast austenitic stainless steel. *Materials Science and Engineering: A*, *526*(1–2), 244–249. https://doi.org/10.1016/J.MSEA.2009.07.044

Krupp, U., West, C., & Christ, H. J. (2008). Deformation-induced martensite formation during cyclic deformation of metastable austenitic steel: Influence of temperature and carbon content. *Materials Science and Engineering: A*, *481–482*(1-2 C), 713–717. https://doi.org/10.1016/J.MSEA.2006.12.211

Kumar, A., & Singhal, L. K. (1989). Effect of strain rate on martensitic transformation during uniaxial testing of AISI-304 stainless steel. *Metallurgical Transactions A 1989 20:12*, *20*(12), 2857–2859. https://doi.org/10.1007/BF02670178

Lee, J.-C., Noh, Y., Kim, N.-S., Park, K. B., Kim, H., Cho, H.-H., Park, H.-K., Jun, T.-S., & Park, C.-S. (2022). *Effect of Texture and Temperature on Strain-Induced Martensitic Transformation in 304 Austenitic Stainless Steel*. https://doi.org/10.1002/srin.202200243

Liu, J., Chen, C., Feng, Q., Fang, X., Wang, H., Liu, F., Lu, J., & Raabe, D. (2017). Dislocation activities at the martensite phase transformation interface in metastable austenitic stainless steel: An in-situ TEM study. *Materials Science and Engineering: A*, *703*, 236–243. https://doi.org/10.1016/J.MSEA.2017.06.107

Mediratta, S. R., Ramaswamy, V., & Rama Rao, P. (1986). Two stage cyclic work hardening and two slope coffin-manson relationship in dual phase steels. *Scripta Metallurgica*, *20*(4), 555–558. https://doi.org/10.1016/0036-9748(86)90253-X

Nagy, E., Mertinger, V., Tranta, F., & Sólyom, J. (2004). Deformation induced martensitic transformation in stainless steels. *Materials Science and Engineering: A*, *378*(1–2), 308–313. https://doi.org/10.1016/J.MSEA.2003.11.074

P. Kuznetsov, V., & V. Kosareva, A. (2023a). Increase of Wear and Heat Resistance of the AISI 304 Steel Surface Layer by Multi-Pass Nanostructuring Burnishing. *Journal of Materials and Engineering*, *1*(2), 55–61. https://doi.org/10.61552/jme.2023.02.001

Paul, S. K., Stanford, N., & Hilditch, T. (2018). Austenite plasticity mechanisms and their behavior during cyclic loading. *International Journal of Fatigue*, *106*, 185–195. https://doi.org/10.1016/J.IJFATIGUE.2017.10.005

Pegues, J. W., Shao, S., Shamsaei, N., Schneider, J. A., & Moser, R. D. (2017). Cyclic strain rate effect on martensitic transformation and fatigue behaviour of an austenitic stainless steel. *Fatigue & Fracture of Engineering Materials & Structures*, *40*(12), 2080–2091. https://doi.org/10.1111/FFE.12627

Radhakrishnan, V. M. (1992). On the bilinearity of the Coffin-Manson low-cycle fatigue relationship. *International Journal of Fatigue*, *14*(5), 305–311. https://doi.org/10.1016/0142-1123(92)90481-Q

Rowcliffe, A. F., Zinkle, S. J., Stubbins, J. F., Edwards, D. J., & Alexander, D. J. (1998). Austenitic stainless steels and high strength copper alloys for fusion components. *Journal of Nuclear Materials*, *258–263*(PART 1 A), 183–192. https://doi.org/10.1016/S0022-3115(98)00333-X

Singh Wadhwa, A., & Chauhan, A. (2023b). An Overview of the Mechanical and Tribological Characteristics of Non - Ferrous Metal Matrix Composites for Advanced Engineering Applications. *Tribology in Industry*, 45(1), 51–80. https://doi.org/10.24874/ti.1359.08.22.12

Talonen, J., & Hänninen, H. (2007). Formation of shear bands and strain-induced martensite during plastic deformation of metastable austenitic stainless steels. *Acta Materialia*, *55*(18), 6108–6118. https://doi.org/10.1016/J.ACTAMAT.2007.07.015

Talonen, Juho, Nenonen, P., Pape, G., & Hänninen, H. (2005). Effect of strain rate on the strain-induced γ, → α′-martensite transformation and mechanical properties of austenitic stainless steels. *Metallurgical and Materials Transactions A: Physical Metallurgy and Materials Science*, *36 A*(2), 421–432. https://doi.org/10.1007/S11661-005-0313-Y

Weiß, A., Gutte, H., & Scheller, P. R. (2006). Deformation induced martensite formation and its effect on Transformation Induced Plasticity (TRIP). *Steel Research International*, *77*(9–10), 727–732. https://doi.org/10.1002/SRIN.200606454

Yamaguchi K, Kanazawa K. Electron microscope on deformati... - Google Scholar. (n.d.).

Chandra Kant
National Institute of Technology
Srinagar,
Srinagar,
India
chandra07phd17@nitsri.ac.in
ORCID 0009-0001-7102-0223

Gulam Ashraful Harmain
National Institute of Technology
Srinagar,
Srinagar,
India
gharmain@nitsri.ac.in
ORCID 0000-0002-7912-5724